CrossMark

ORIGINAL PAPER

Electrochemical indirect competitive immunoassay for ultrasensitive detection of zearalenone based on a glassy carbon electrode modified with carboxylated multi-walled carbon nanotubes and chitosan

Wei Xu[1] · Ying Qing[1] · Shuai Chen[1] · Jun Chen[1] · Zhen Qin[1] · JingFu Qiu[1] (iD) ·
ChaoRui Li[1]

Abstract The authors describe an electrochemical immunoassay for ultrasensitive detection of the mycotoxin zearalenone (ZEA). A nanocomposite was prepared from carboxy-functionalized multi-walled carbon nanotubes and chitosan (cMWCNTs/Chit). The morphology and electrochemical performance of the materials was characterized by field-emission scanning electron microscopy, atomic force microscopy, differential pulse voltammetry, cyclic voltammetry, and electrochemical impedance spectroscopy. In this assay, ZEA–BSA conjugated covalently to activated cMWCNTs/Chit film, then the indirect competition between ZEA–BSA and free ZEA when immobilization of excess anti-ZEA. The secondary antibody is labeled with the enzyme alkaline phosphatase which can hydrolyze the substrate 1-naphthylphosphate to produce 1-naphthol which gives a stable and strong anodic electrochemical signal at a low working voltage of 0.3 V (vs. Ag/AgCl). The use of the modified GCE results in a strongly enhanced electrochemical current response. Compared with conventional methods, the established immunosensor exhibited a high level of sensitivity. Under optimal conditions, this immunoassay can quantify ZEA in the 10 pg·mL−1 to 1000 ng·mL−1 concentration range with a detection limit of 4.7 pg·mL−1 and the sensitivity is 0.51 μA·μM−1·cm−2. The method was applied to the determination of ZEA in cereal and feedstuff samples. Results showed satisfactory recovery and good consistency with high-performance liquid chromatography. Therefore, the indirect competitive electrochemical immunosensor provide a viable tool based on bioanalysis.

Introduction

Zearalenone (ZEA) is a mycotoxin that is produced by several *Fusarium* species with a high estrogenic activity in vitro and in vivo [1] and can cause serious damage to the reproductive systems of humans and animals [2]. ZEA reaches cereal grains, feedstuff, and animal products through fungal [3] and water contamination. Regarding biological systems, ZEA exerts adverse effects such as hepatotoxicity, hematological toxicity, genotoxicity, immunotoxicity and neurotoxicity [4]. The European Food Safety Authority claims that the tolerable daily intake of ZEA should not exceed 0.25 mg·kg^{-1} [5]. Thus, developing a sensitive and reliable detection method to prevent detrimental effects to human health is vital. Various analytical strategies and techniques have been reported for the quantitative monitoring of ZEA in food and fodder, including high-performance liquid chromatography (HPLC) coupled with mass spectrometry [6], lateral flow immunoassays [7], and enzyme-linked immunosorbent assays [8]. These methods can detect ZEA with high accuracy and robustness. However, such procedures require expensive apparatuses, sophisticated sample preparation, intensive labor, and a high investment; therefore, on-line determinations are restricted. For food safety analysis, electrochemical immunosensors are used in portable devices and point-

✉ JingFu Qiu
jfqiu@126.com

✉ ChaoRui Li
crli@cqmu.edu.cn

[1] School of Public Health and Management, Chongqing Medical University, Chongqing 400016, China

of-care applications [9]. Compared with the direct and sandwich methods, the indirect competition assay can provide high sensitivity and selectivity, particularly for small molecules (such as ZEA), due to a run that is based on a competitive principle in a hydrodynamically focused fluid stream [10]. Thus, such sensing elements show significant potential and prevent the drawbacks of traditional methods.

Graphene [11], cellulose nanowhiskers [12], gold-dotted nanoparticles [13], and carbon nanotubes (CNTs) [14] represent nanomaterials that are considered efficient and facile solutions [15] in constructing typical sensing interfaces. Among these materials, CNTs and multi-walled carbon nanotubes (MWCNTs) have attracted considerable interest in the areas of supramolecular nano-bio-assembly and nano-biosensor fabrication [16]. Carboxylic-group-functionalized MWCNTs (cMWCNTs) are extensively applied because these nanotubes allow for the rapid and direct electron transfer in a wide range of electron active species and electrode materials. Nevertheless, the agglomeration of cMWCNTs in aqueous solutions restricts their application [17]. Chitosan (Chit), a polymer abound with amino groups, exhibits good film-forming properties [18]. Consequently, Chit presents a suitable matrix for immobilizing bioactive molecules and constructing biosensors [19]. cMWCNTs can substantially improve the properties of polymers with low loadings [20]. cMWCNTs/Chit nanocomposites can be formed by integrating cMWCNTs with Chit through their carboxy and amino groups. This formation not only reduces the impedance [21] but also improves the electrochemical signals [22]. The sensitivity is highly related to the current signal difference, which is caused by analytes, and is significantly affected by the immunosensor conductivity [23]. Thus, cMWCNTs/Chit can increase the sensitivity of electrochemical immunosensors.

In this study, we developed an electrochemical immunosensor that is based on the indirect competitive format, where cMWCNTs/Chit acts as an electrotransfer mediator, and α-naphthyl phosphate (α-NP) serves as the enzyme substrate for ZEA detection in cereal grains and fodder. First, ZEA-bovine serum albumin (ZEA–BSA) was covalently conjugated to the activated cMWCNTs/Chit film; then, the indirect competition occurred between ZEA–BSA and free ZEA during the immobilization of excess anti-ZEA. After incubation with the AP-anti-antibody, DPV was conducted when the α-NP enzyme substrate was added to the diethanolamine (DEA) buffer as the redox mediator. In this methodology, the blocking step was unnecessary because the antigens, ZEA–BSA, were immobilized on cMWCNTs/Chit; therefore, a substantial amount of BSA that was coated onto a surface eliminated the non-specific binding effect and blocked the remaining active sites [24]. Experimental studies showed that electrodes modified with cMWCNTs/Chit nanocomposites exhibited excellent sensing performance during ZEA detection.

Experimental

Reagents and apparatus

ZEA–BSA, ZEA, anti-ZEA, a negative corn sample and ZEA immunoaffinity columns were purchased from Beijing Huaan Magnech Biotechnology Co., Ltd. (Beijing, China, http://www.magnech.com). cMWCNTs (diameter, <8 nm) were purchased from XFNANO Technology Co., Ltd. (Nanjing, China, http://www.xfnano.com). Samples (corn, wheat and fodder) that were naturally contaminated with ZEA were purchased from Qingdao Pribolab Biotechnology Co., Ltd. (Qingdao, China, http://www.pribolab.cn). Chitosan, alkaline phosphatase (AP)-anti-antibody, N-hydroxysuccinimide (NHS), α-NP and 1-ethyl-3-(3-dimethylaminopropyl)carbodiimide hydrochloride (EDC) were obtained from Sigma-Aldrich (USA, http://www.sigmaaldrich.com). A 0.1 M phosphate buffer (pH 7.4) was utilized as the working buffer. A diethanolamine (DEA) buffer (pH 9.6) that contained 0.1 M DEA, 1 M $MgCl_2$ and 0.1 M KCl was used as the reaction solution, and the pH was adjusted to 9.6 with 0.1 M hydrochloric acid. All other reagents were of analytical grade and used without further purification. All aqueous solutions were prepared using Millipore-Q water ($\geq$18 M$\Omega\cdot$cm).

Electrochemical measurements, including cyclic voltammetry (CV), differential pulse voltammetry (DPV), and electrochemical impedance spectroscopy (EIS), were all performed on an AUTOLAB PGSTAT302 N electrochemical workstation (METROHM AUTOLAB B.V., The Netherlands, www.metrohm-autolab.com) with a conventional three-electrode configuration. It consisted of a platinum wire as auxiliary electrode, Ag/AgCl (with 3 M KCl) as reference electrode, and 3 mm diameter glassy carbon electrode (GCE) modified by cMWCNTs/Chit (geometrical surface area of all working electrodes =0.07 cm^2) were purchased from Gaoss union Technology Co., Ltd. (Wuhan, China, http://www.gaossunion.com) as working electrode. Field emission scanning electron microscopy (FE-SEM) images were obtained using a Hitachi S4800 system (Hitachi Limited, Japan). Atomic force microscopy (AFM) images were acquired by Bruker Dimension icon (USA). All measurements were performed at room temperature under ambient conditions.

Electrochemical measurements

All electrochemical experiments were conducted in an electrochemical cell containing a conventional three-electrode chemical system. CV was performed in a 5.0 mM $[Fe(CN)_6]^{3-/4-}$ solution that contained 0.1 M KCl from −0.1 V to +0.6 V at a scan rate of 0.1 V s^{-1}. EIS was performed in 5.0 mM $[Fe(CN)_6]^{3-/4-}$ that contained 0.1 M KCl in a frequency range from 0.1 Hz to 10^5 Hz. DPV was conducted in a 0.1 M fresh DEA buffer (pH 9.6) that contained 0.75 mg·mL^{-1} α-NP. The potential ranged from −0.05 V to +0.55 V at

a scan rate of 0.025 V s^{-1}. The following DPV parameters were utilized: the modulation amplitude was 0.07 V, the modulation time was 0.05 s, and the interval time was 0.2 s.

Synthesis of cMWCNTs/Chit

cMWCNTs/Chit nanocomposites were prepared following the procedure from a previous study [25] with minor modifications. First, 50 mg of chitosan powder was dispersed in 10 mL of a 1% acetic acid solution, vigorously shaken for 2 min and then sonicated for 1 h. Second, 40 mg of fine powder of the cMWCNTs was dispersed in the prepared Chit solution. Third, the solution was sonicated for at least 2 h until the homogeneous dispersion of the cMWCNTs/Chit nanocomposites was achieved. Finally, the prepared cMWCNTs/Chit dispersion liquid was stored at 4 °C until further use.

Fabrication of the electrochemical immunosensor

Bare GCEs were successively polished into mirrors using both 0.3 μm and 0.05 μm alumina slurries on microcloth pads. The electrodes were then subjected to ultrasonic cleaning in ultrapure water, nitric acid and acetone (1:1, *v*/*v*) for several minutes. After drying in nitrogen at room temperature, 2 μL of the 1 mg·mL^{-1} cMWCNTs/Chit dispersion was coated onto the surface of the prepared GCEs.

EDC/NHS is a moderate cross-linking reagent. The amino of cMWCNTs/Chit integrated with the carboxy of BSA on the surface of the GCE using EDC/NHS. Subsequently, cMWCNTs/Chit/GCE was treated with 50 μL of freshly prepared 0.4 M EDC-0.1 M NHS for 1 h at 37 °C. Next, cMWCNTs/Chit/GCE was thoroughly rinsed with a 0.1 M phosphate buffer (pH 7.4) solution. After washing as previously described, 10 μL of 1 μg·mL^{-1} ZEA–BSA, which was a diluted phosphate buffer solution, was quickly dropped onto the GCE and the electrode was incubated for 1.5 h at 37 °C. The electrochemical immunosensor was successfully fabricated.

For the competition assay, 5 μL of diluted anti-ZEA (1:50, *v*/*v*) was blended with 5 μL of the ZEA standard solution with concentrations ranging from 0 to 1000 ng·mL^{-1}. After 30 min of competition in a centrifuge tube, 10 μL of miscible competition fluid was deposited onto the electrode surface that was modified with ZEA–BSA and the electrode was incubated for 1.5 h at 37 °C. During incubation, immobilized ZEA–BSA competed with the ZEA standard solution for anti-ZEA. The electrode was washed with a phosphate buffer solution at least three times after each incubation step. Subsequently, the prepared immunosensor was incubated with 10 μL of AP-anti-antibody (1:200, *v*/*v*) for 1.5 h at 37 °C. After thorough rinsing with the DEA buffer, the resulting electrode was immersed into a freshly prepared DEA solution that contained 0.75 mg·mL^{-1} of α-NP for the DPV measurements.

Sample preparation

Food samples were purchased from Beijing Huaan Magnech Biotechnology Ltd. Co. (Beijing, China, http://magnech.bioon. com.cn). The ZEA-free corn sample was prepared as follows. First, a 20-g corn sample was added to 100 mL of deionized water and acetonitrile (1:4, *v*/*v*) in a plastic centrifuge tube. Then, the ZEA-free corn samples were spiked with appropriate concentrations of ZEA and vigorously shaken for 20 min. Next, the mixture was centrifuged for 10 min at 12,000 rpm, and the supernatant color changed from colorless to canary yellow. The supernatant was filtered through a fast qualitative filter paper to remove solid matter. Next, 10 mL of filtrate was carefully diluted with 40 mL of the phosphate buffer solution and 0.05% Tween-20, which was used for the antigen-antibody reaction. The extract was filtered through a microfiber glass filter (Whatman 934-AH) to remove solid particles. Subsequently, 25 mL of the filtrate was filtered through an immunoaffinity column at a flow rate of 1 drop/s and then washed twice with 10 mL of deionized water to remove interfering compounds. Enriched ZEA was eluted with 1 mL of methanol and collected. Pretreatments of corn, wheat, and cattle fodder with ZEA were the same as those of the ZEA-free corn samples. Finally, the sample solution was diluted to appropriate concentrations and stored at −20 °C for subsequent use.

Results and discussion

Choice of material

cMWCNTs have an excellent electrical conductivity and have emerged as a low-cost interesting carbonaceous nanomaterial [26]. Important sensor parameters such as selectivity, sensitivity, reproducibility and detection limit are significantly improved with cMWCNTs-based nanocomposites. In contrast, the studies of Karimi et al. revealed that Chit exhibits an excellent film-forming ability that can decrease the aggregation of cMWCNTs. During the past 20 years, a considerable amount of work has been reported on chitosan and its potential use in various bioapplications. Therefore, we have prepared cMWCNTs/Chit and demonstrated its applicability in ZEA sensing. Our studies revealed that cMWCNTs/Chit nanocomposites showed excellent sensing attributes towards ZEA in cereal grains and fodder samples that were measured in the laboratory.

Design of a ZEA immunosensor

Scheme 1 illustrates the overall preparation of the immunosensors. The GCE was modified with a functionalized cMWCNTs/Chit nanocomposite film (cMWCNTs/Chit/GCE) to amplify the immunosensor signal and reduce the limit of

Scheme 1 Schematic of reaction and protocols involved in preparation of electrochemical GCE immunosensor for ZEA
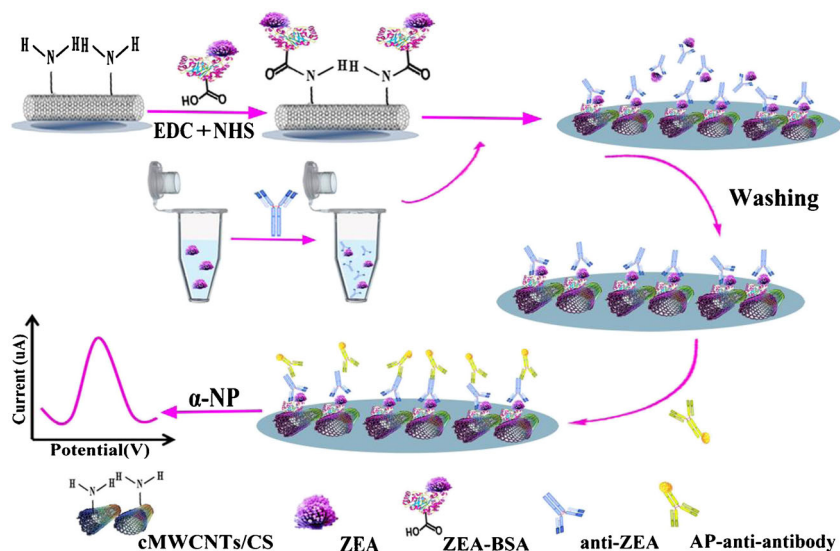
detection (LOD). This enhancement is attributed to desirable physicochemical and electrical properties and the large ratio surface area of cMWCNTs/Chit. ZEA–BSA was covalently conjugated to the activated cMWCNTs/Chit film. In the competitive stage, after the immobilization of excess anti-ZEA and the reaction between ZEA–BSA and antigens in solution, the remaining unconjugated anti-ZEA attached to the ZEA–BSA-modified electrode. The quantitation of ZEA was performed with a secondary antibody, AP-anti-antibody, and DPV was conducted when the α-NP enzyme substrate was added as the redox mediator. A linear relationship existed between the DPV peak currents and the logarithm of ZEA concentration. Therefore, the concentrations of ZEA in the samples were successfully monitored.

Morphological characterization of cMWCNTs/Chit and the stepwise modification of the immunosensor

FE-SEM and AFM were performed to characterize nanocomposites on the immunosensor surface and to demonstrate variations in physical properties and sizes of these nanocomposites during immunosensor synthesis. Fig. 1 shows FE-SEM images of the surface morphologies of cMWCNTs and cMWCNTs/

Chit composite powders. Without Chit (Fig. 1a), cMWCNTs demonstrated curved and coiled tubular structures because of their large surface area [17]. The tubes formed three-dimensional (3D) networks with a porous structure and agglomerated with one another. After Chit addition (Fig. 1b), the Chit contained a substantial amount of amino groups that dramatically increased the dispersion of cMWCNTs in a water solution and prevented the agglomeration of cMWCNTs [17]. Consequently, the nanomaterials constituted a highly close-knit 3D network. The cMWCNTs/Chit nanocomposites exhibited a homogeneous distribution and were further incorporated into the polymers [27].

Fig. 2 shows typical AFM topographical images of the stepwise modification of immunosensors [28]. Fig. 2a shows the accumulation of a packed cMWCNTs/Chit monolayer with ridged and tubular topography. This figure provides evidence of abundant binding sites on the cMWCNTs/Chit surface with covalently bound ZEA–BSA with a height of 62.24 nm. The electrode topography changed to a typically smooth morphology as result of the covalent linkage of ZEA–BSA to cMWCNTs/Chit. In Fig. 2b, the layer height significantly increased to a height of 367.87 nm. This outcome can be attributed to a blocking of non-specific binding sites and

Fig. 1 FE-SEM images of a cMWCNTs and b cMWCNTs/Chit nanocomposite
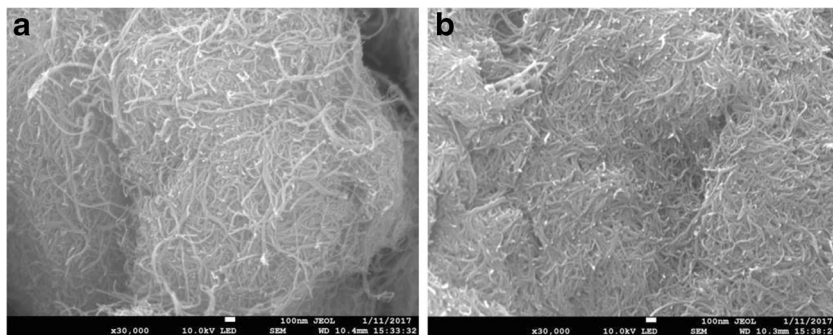
Fig. 2 AFM images of a
cMWCNTs/Chit, b ZEA–BSA/
cMWCNTs/Chit, c anti-ZEA/
ZEA–BSA/cMWCNTs/Chit d
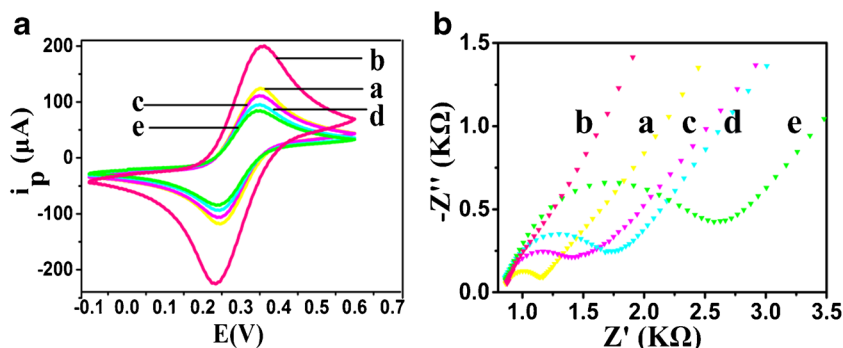AP-anti-antibody/anti-ZEA/
ZEA–BSA/cMWCNTs/Chit
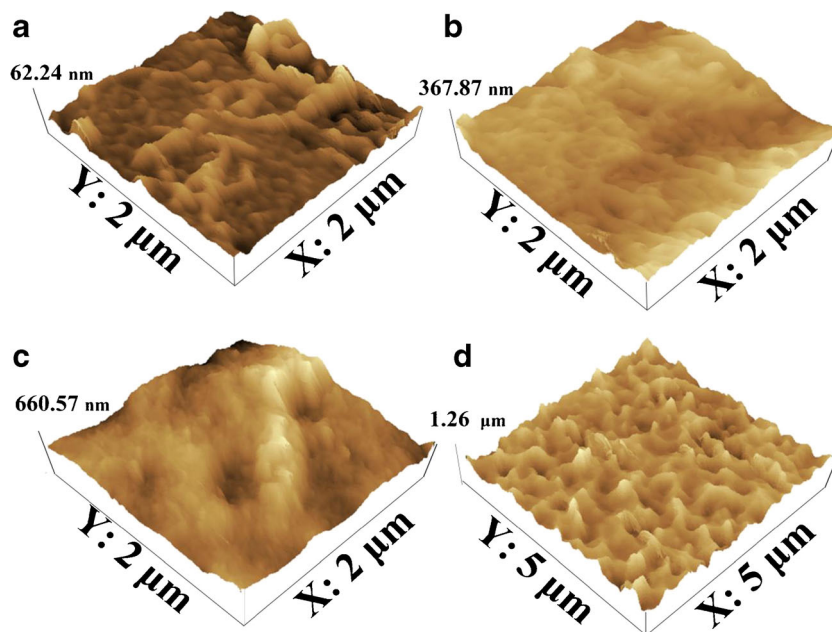
the formation of a uniform immunosensor surface. Then, the promontory height on the sensor surface significantly increased after the interaction of the anti-ZEA and anti-antibody. This phenomenon is due to the specific binding of the antibody and antigen with heights on the sensor surface of 660.57 nm and 1.26 μm, respectively. (Figs. 2c–d).

Electrochemical characterization of various modified electrodes

CV and EIS measurements were performed after each incubation step to examine interfacial properties of the modified electrodes during fabrication. In Fig. 3a, a bare GCE curve exhibited a well-defined reversible redox peak. In curve b of the cMWCNTs/Chit-modified electrode, the redox peak current significantly increased because cMWCNTs/Chit facilitated electron transfer [29]. After applying the ZEA–BSA coating, the peak current remarkably declined (curve c) because

ZEA–BSA modified the surface covering of cMWCNTs/Chit/GCE and induced the decrease in conductivity. Consequently, antigen binding causes a shielding effect and a reduction of the electron transfer rate. As expected, the peak current continuously dropped after the interaction of anti-ZEA with ZEA–BSA (curve d) because the antigen-antibody reaction produced a high electric resistance, and the antigen functioned as an inert-electron-and mass-transfer-blocking layer [9]. Finally, the peak current was reduced to a minimum because of the specific binding of AP-anti-antibody to anti-ZEA (curve e). This result is attributed to the production of immunocomplexes that blocked active sites of the mediator and decreased its electron transfer capability. CV results agree with those of EIS (Fig. 3b). In EIS, the semicircle diameter equals that of the electron transfer resistance (Ret), which controls the electron transfer kinetics of redox probes at the electrode interface [24]. Consistent CV and EIS, the results illustrate the successful construction of immunosensors.

Fig. 3 a CV and **b** EIS responses of different electrodes in 0.1 M KCl aqueous solution containing 5.0 mM $[Fe(CN)_6]^{3-/4-}$: (a) bare GCE, (b) cMWCNTs/Chit/GCE, (c) ZEA–BSA/cMWCNTs/Chit/GCE, (d) anti-ZEA/ZEA–BSA/cMWCNTs/Chit/GCE, and (e) AP-anti-antibody/anti-ZEA/ZEA–BSA/cMWCNTs/Chit/GCE
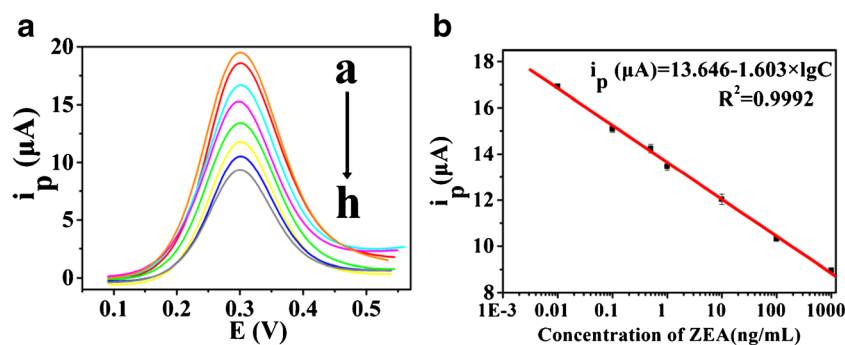
Fig. 4 **a** Typical DPV response of designed immunosensor to ZEA concentrations of (a) 0, (b) 10 pg·mL^{-1}, (c) 100 pg·mL^{-1}, (d) 500 pg·mL^{-1}, (e) 1 ng·mL^{-1}, (f) 10 ng·mL^{-1}, (g) 100 ng·mL^{-1}, (h) 1 μg·mL^{-1}; **b** plot of DPV current with respect to logarithms of different ZEA concentrations (Error bars represent average standard errors for three measurements)

Optimization of experimental conditions

Certain external experimental parameters influence performance of fabricated electrochemical immunosensor, and they should be optimized to achieve high sensitivity, high selectivity, and low detection limit. These parameters include (a) concentration of ZEA–BSA, (b) dilution ratio of anti-ZEA, (c) dilution ratio of AP-anti-antibody, (d) concentration of α-NP, (e) pH value of supporting electrolyte, and (f) competition time. The results are presented in the Electronic Supporting Material (Fig. S1) The following experimental conditions yielded optimal results: (a) ZEA–BSA concentration of 1 μg·mL^{-1}, (b) anti-ZEA dilution ratio of 1:100, (c) AP-anti-antibody dilution ratio of 1:200, (d) α-NP concentration of 0.75 mg·mL^{-1}; (e) pH value of 9.6; (f) competition time of 30 min.

Analytical performance of the electrochemical immunosensor

Sensitivity of the immunosensor for ZEA determination

Under optimized experimental conditions, effects of different concentrations of ZEA on analytical capability were examined by DPV in DEA (pH 9.6). In Fig. 4a, redox peak currents clearly decline with increasing concentrations of ZEA. The results indicate the successful incorporation of ZEA with

anti-BSA; therefore, the AP-anti-antibody also cannot interact. Calibration plots between the DPV response and the logarithm of ZEA concentration display a good linear relationship from 0.001 pg·mL^{-1} to 1000 ng·mL^{-1} (Fig. 4b) and fit the linear regression equation $i_p(A) = 13.64067 - 1.60317 \times \log C_{ZEA}$ (ng·mL^{-1}), $R^2 = 0.9992$. The error bars represent the standard deviation (SD) of three measurements. The detection limit was 4.7 pg·mL^{-1} and was estimated to be three times that of the SD of the blank sample/slope. The sensitivity was 0.51 μA·μM^{-1}·cm^{-2}. The immunosensor achieved a wider linear dynamic range with an acceptable detection limit compared with other existing ZEA detection methods, as shown in Table 1.

Specificity of the immunosensor

The specificity of the immunosensor was evaluated using 1 ng·mL^{-1} ZEA and a 100-fold mass ratio of competitors (100 ng·mL^{-1}), including deoxynivalenol (DON), ochratoxin (OTA), fumonisin B$_1$ (FB$_1$), aflatoxins B$_1$ (AFB$_1$) and a mixture of all abovementioned mycotoxins compounds (Mix). Fig. 5 presents the current responses for six types of samples and a blank. First, the current responses of DON, OTA, FB$_1$, and AFB$_1$ did not exhibit significant differences from the blank sample. Second, as shown in Mix current response and compared to only 1 μg·mL^{-1} ZEA, the current responses

Table 1 Comparison of linear and detection limits of designed immunosensor and other ZEA detection methods

Methods	Linear dynamic range (ng·mL^{-1})	Limit of detection (ng·mL^{-1})	Reference
Electrochemical immunosensing	0.004–9.5	0.002	[30]
Electrochemical immunosensing	0.005–50	0.0015	[31]
Electrochemical immunosensing	0.05–50	0.016	[32]
Electrochemical immunosensing	0.03–35	0.01	[33]
HPLC-MS /MS	0.54–42.5	0.04	[6]
Multiplex lateral flow immunoassay	—	0.42	[7]
Recombinant cell fluorescence biosensor	10–100	3.2	[34]
Enzyme-linked immunosorbent assay	0.07–2.41	0.04	[35]
Electrochemical immunosensor	0.01–1000	0.0047	This work
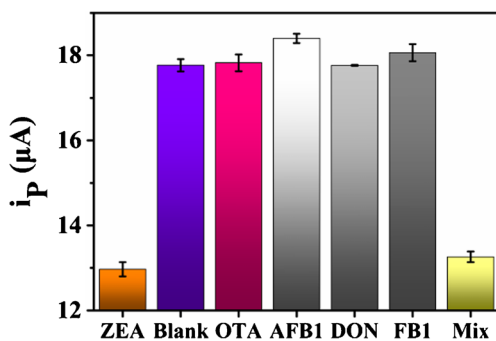
Fig. 5 Specificity of electrochemical immunosensor for 1 ng·mL^{-1} ZEA, blank, 100 ng·mL^{-1} of OTA, AFB1, DON, FB1 and mixture

still did not significantly vary when the concentrations of other mycotoxins increased to 100 ng·mL^{-1} and were combined with 1 μg·mL^{-1} ZEA. The results indicate a non-specific interaction of other toxins on the electrochemical immunosensor. These foreign mycotoxins had a negligible effect on the ZEA determination.

Reproducibility and stability of the designed immunosensor

In Table S1, the reproducibility of the electrochemical immunosensor was evaluated for detecting ZEA with concentrations of 10 pg·mL^{-1}, 1 ng·mL^{-1}, and 1 μg·mL^{-1} in five separate electrodes that belong to the same batch but were independently welded by the same assembly procedure. These separate electrodes exhibited similar DPV responses. The relative SD for ZEA concentrations of 10 pg·mL^{-1}, 1 ng·mL^{-1}, and 1 μg·mL^{-1} were 2.43%, 2.39%, and 1.88%, respectively. The results demonstrate that the fabricated immunosensor exhibits an acceptable reproducibility. The stability represents another important parameter in the quantitative detection of an immunosensor. Fig. S2 shows that the DPV current for 2.9% activity was retained after storing the sensor under dry conditions at 4 °C for 15 days.

Accuracy of ZEA in the samples

The applicability and reliability of the immunosensor for the determination of ZEA in cereal grains and fodder were evaluated. The negative corn sample was spiked with ZEA at 0, 10, 100, 1000, and 10,000 μg·kg^{-1} concentrations, whereas corn, wheat and fodder samples that are naturally contaminated with ZEA were tested by the designed method and conventional HPLC. In Table 2, the recovery rates of the spiked corn samples range from 94% to 106.4%. At the same time, the relative errors between the results of the two methods range from 0.72% to 6.06% (naturally contaminated corn sample), 0.81% to 1.02% (naturally contaminated wheat sample), and 0.25% to 1.26% (naturally contaminated fodder sample). These results demonstrated that the electrochemical immunosensor can detect ZEA in various foods. Consequently, the immunosensor is highly promising and presents an innovative method for the determination of ZEA.

Conclusions

In this work, an ultrasensitive electrochemical immunosensor for ZEA was successfully constructed using an indirect competitive format and eliminating the blocking step. The immunosensor utilized the AP enzymatic reaction and cMWCNTs/Chit to achieve signal generation and amplification. Under optimal conditions, this immunosensor exhibited a wide linear range from 0.001 ng·mL^{-1} to 1000 ng·mL^{-1} and low detection limit of 4.7 pg·mL^{-1}. The fabricated biosensor was successfully applied to the detection of ZEA in cereal grains and fodder and showed satisfactory recovery and good agreement with the conventional HPLC method. However, one limitation is that the method involves several time-consuming steps or a 3.5 h analysis time, which will be addressed in future work.

Table 2 Application of immunosensor for ZEA determination in cereal grains and fodder

Spiked sample no.	Added (μg·kg^{-1})	Electrochemical immunosensor (μg·kg^{-1})[a]	Recovery (%)
1	0	2.29 ± 0.3	0
2	10	9.40 ± 1.22	94
3	100	101.18 ± 27.08	101.2
4	1000	1064.73 ± 121.36	106.4
5	10,000	9983.26 ± 823.51	99.8
Naturally contaminated corn samples[b]			Relative error (%)
1	16.49	16.61 ± 4.99	0.72
2	0.33	0.35 ± 0.17	6.06
Naturally contaminated wheat samples[b]			Relative error (%)
1	245	247 ± 32.67	0.81
2	4.9	4.85 ± 0.04	1.02
Naturally contaminated fodder samples[b]			Relative error (%)
1	47.41	47.29 ± 6.03	0.25
2	1.58	1.56 ± 0.17	1.26

[a] Mean ± SD of three mesurements

[b] The results were obtained by HPLC and this work

References

1. Mally A, Solfrizzo M, Degen GH (2016) Biomonitoring of the mycotoxin Zearalenone: current state-of-the art and application to human exposure assessment. Arch Toxicol 90(6):1–12

2. Rong Y, Wang YM, Li Z, Zhao ZM, Zhao J, Peng SQ (2016) Prepubertal exposure to an oestrogenic mycotoxin zearalenone induces central precocious puberty in immature female rats through the mechanism of premature activation of hypothalamic kisspeptin-GPR54 signaling. Molecular & Cellular Endocrinology 437(C):62–74

3. Long M, Yang S, Zhang W, Zhang Y, Li P, Guo Y, Wang Y, Chen X, He J (2016) The influence of selenium yeast on hematological, biochemical and reproductive hormone level changes in kunming mice following acute exposure to zearalenone. Biol Trace Elem res 174(2):1–7

4. Zinedine A, Soriano JM, Moltó JC, Mañes J (2007) Review on the toxicity, occurrence, metabolism, detoxification, regulations and intake of zearalenone: an oestrogenic mycotoxin. Food & Chemical Toxicology an International Journal Published for the British Industrial Biological Research Association 45(1):1–18

5. EFSA (2011) Scientific opinion on the risks for public health related to the presence of zearalenone in food. EFSA j 9(6):2197

6. Zhao H, Chen X, Shen C, Qu B (2017) Determination of 16 mycotoxins in vegetable oils using a QuEChERS method combined with high-performance liquid chromatography-tandem mass spectrometry. Food Additives & Contaminants Part a, Chemistry, Analysis, Control, Exposure & Risk Assessment 34(2):255–264

7. Chen Y, Chen Q, Han M, Zhou J, Gong L, Niu Y, Zhang Y, He L, Zhang L (2016) Development and optimization of a multiplex lateral flow immunoassay for the simultaneous determination of three mycotoxins in corn, rice and peanut. Food Chem 213:478–484

8. Tima H, Rácz A, Guld Z, Mohácsifarkas C, Kiskó G (2016) Deoxynivalenol, zearalenone and T-2 in grain based swine feed in Hungary. Food Addit Contam part B Surveill 1-6

9. Kavosi B, Salimi A, Hallaj R, Moradi F (2015) Ultrasensitive electrochemical immunosensor for PSA biomarker detection in prostate cancer cells using gold nanoparticles/PAMAM dendrimer loaded with enzyme linked aptamer as integrated triple signal amplification strategy. Biosens Bioelectron 74:915–923

10. Kong W, Xiao C, Ying G, Liu X, Zhao X, Wang R, Li W, Yang M (2017) Magnetic microspheres-based cytometric bead array assay for highly sensitive detection of ochratoxin a. Biosens Bioelectron 94:420

11. Zheng P, Ma T, Ma X (2013) Fabrication and properties of starch-grafted graphene nanosheet/plasticized-starch composites. Ind Eng Chem res 52(39):14201–14207

12. Xie F, Pollet E, Halley PJ, Avérous L (2013) Starch-based nano-biocomposites. Prog Polym Sci 38(10–11):1590–1628

13. Edozie SC, Milua M, Lindsay W, Candice R, Tesfaye W, Baker PGL, Iwuoha EI (2015) Application on gold nanoparticles-dotted 4-nitrophenylazo graphene in a label-free impedimetric deoxynivalenol immunosensor. Sensors 15(2):3854–3871

14. Jose J, De SK, Alma'Adeed MAA, Dakua JB, Sreekumar PA, Sougrat R, Al-Harthi MA (2014) Compatibilizing role of carbon nanotubes in poly(vinyl alcohol)/starch blend. Starch-Starke 67(1–2):147–153

15. Qian D, Chang PR, Zheng P, Ma X (2012) Preparation and characterization of plasticized starch/carbon black-oxide nanocomposites. Ind Eng Chem res 51(23):7941–7947

16. Hong J, Zhao YX, Xiao BL, Moosavi-Movahedi AA, Ghourchian H, Sheibani N (2013) Direct electrochemistry of hemoglobin immobilized on a functionalized multi-walled carbon nanotubes and gold nanoparticles nanocomplex-modified glassy carbon electrode. Sensors 13(7):8595

17. Liu Z, Zhao L, Chen M, Yu J (2011) Effect of carboxylate multi-walled carbon nanotubes on the performance of thermoplastic starch nanocomposites. Carbohydr Polym 83(2):447–451

18. Karimi AR, Khodadadi A (2016) Mechanically robust 3D nanostructure chitosan-based hydrogels with autonomic self-healing properties. ACS Appl Mater Interfaces 8(40):27254

19. Pillai CKS, Paul W, Sharma CP (2009) Chitin and chitosan polymers: chemistry, solubility and fiber formation. Prog Polym Sci 34(7):641–678

20. Gou Z, Xu D, Dong Q, Wu X (2016) Comparison studies on covalently and non-covalently modified MWNTs using chitosan and their starch nanocomposites. Starch - Stärke 68(3–4):220–229

21. Xu H, Wang L, Luo J, Song Y, Liu J, Zhang S, Cai X (2015) Selective recognition of 5-hydroxytryptamine and dopamine on a multi-walled carbon nanotube-chitosan hybrid film-modified microelectrode array. Sensors 15(1):1008

22. Mally A, Solfrizzo M, Degen GH (2016) Biomonitoring of the mycotoxin Zearalenone: current state-of-the art and application to human exposure assessment. Arch Toxicol 90(6):1281

23. Tang Z, Wang L, Ma Z (2016) Triple sensitivity amplification for ultrasensitive electrochemical detection of prostate specific antigen. Biosens Bioelectron

24. Zhang B, Zhang Y, Liang W, Cui B, Li J, Yu X, Huang L (2016) Nanogold-penetrated poly(amidoamine) dendrimer for enzyme-free electrochemical immunoassay of cardiac biomarker using cathodic stripping voltammetric method. Anal Chim Acta 904:51–57

25. Qing Y, Li C, Yang X, Zhou X, Xue J, Luo M, Xu X, Chen S, Qiu J (2016) Electrochemical immunosensor using single-walled carbon nanotubes/chitosan for ultrasensitive detection of deoxynivalenol in food samples. J Appl Electrochem 46(10):1049–1057

26. Bao J, Hou C, Dong Q, Ma X, Chen J, Huo D, Yang M, Galil KH, Chen W, Lei Y (2016) ELP-OPH/BSA/TiO2 nanofibers/c-MWCNTs based biosensor for sensitive and selective determination of p-nitrophenyl substituted organophosphate pesticides in aqueous system. Biosens Bioelectron 85:935–942

27. Venkatesan J, Qian ZJ, Ryu BM, Kumar NA, Kim SK (2011) Preparation and characterization of carbon nanotube-grafted-chitosan – natural hydroxyapatite composite for bone tissue engineering. Carbohydr Polym 83(2):569–577

28. Izadi Z, Sheikh-Zeinoddin M, Ensafi AA, Soleimanian-Zad S (2016) Fabrication of an electrochemical DNA-based biosensor for Bacillus Cereus detection in milk and infant formula. Biosens Bioelectron 80:582

29. Wang H, Yao S, Liu Y, Wei S, Su J, Hu G (2017) Molecularly imprinted electrochemical sensor based on au nanoparticles in

carboxylated multi-walled carbon nanotubes for sensitive determination of olaquindox in food and feedstuffs. Biosens Bioelectron 87:417–421

30. Wang YK, Yan YX, Mao ZW, Wang HA, Zou Q, Hao QW, Ji WH, Sun JH (2013) Highly sensitive electrochemical immunoassay for zearalenone in grain and grain-based food. Microchim Acta 180(3): 187–193

31. Liu N, Nie D, Tan Y, Zhao Z, Liao Y, Wang H, Sun C, Wu A (2017) An ultrasensitive amperometric immunosensor for zearalenones based on oriented antibody immobilization on a glassy carbon electrode modified with MWCNTs and AuPt nanoparticles. Microchim Acta 184(1):1–7

32. Regiart M, Seia MA, Messina GA, Bertolino FA, Raba J (2015) Electrochemical immunosensing using a nanostructured functional platform for determination of α-zearalanol. Microchim Acta 182(3):531–538

33. Afzali D, Fathirad F (2016) Determination of zearalenone with a glassy carbon electrode modified with nanocomposite consisting of palladium nanoparticles and a conductive polymeric ionic liquid. Microchim Acta 183(9):1–6

34. Ji J, Gu W, Sun C, Sun J, Jiang H, Zhang Y, Sun X (2016) A novel recombinant cell fluorescence biosensor based on toxicity of pathway for rapid and simple evaluation of DON and ZEN. Scientific Reports 6:31270

35. Zhang X, Wang X, Sun M, Zhang X, Song H, Yan Y, Sun J, Li X, Fang W (2015) A magnetic nanoparticle based enzyme-linked immunosorbent assay for sensitive quantification of zearalenone in cereal and feed samples. Toxins 7(10):4216–4231